ACCOUNTS
of chemical research

Concerted Proton–Electron Transfers: Electrochemical and Related Approaches

CYRILLE COSTENTIN, MARC ROBERT, AND JEAN-MICHEL SAVÉANT*

Laboratoire d'Electrochimie Moléculaire, Unité Mixte de Recherche Université - CNRS No 7591, Université Paris Diderot, Bâtiment Lavoisier, 15 rue Jean de Baïf, 75205 Paris Cedex 13, France

RECEIVED ON NOVEMBER 30, 2009

CONSPECTUS

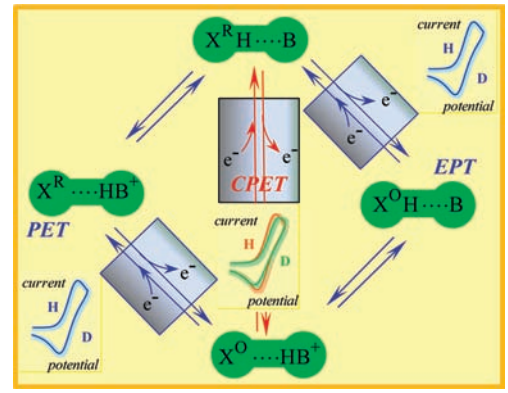

Proton-coupled electron transfers (PCETs) are omnipresent in natural and artificial chemical processes. Given the contemporary challenges associated with energy conversion, pollution abatement, and the development of high-performance sensors, a greater understanding of the mechanisms that underlie the practical efficiency of PCETs is a timely research topic.

In contrast to hydrogen-atom transfers, proton and electron transfers involve different centers in PCET reactions. The reaction may go through an electron- or proton-transfer intermediate, giving rise to the electron–proton transfer (EPT) and the proton–electron transfer (PET) pathways. When the proton and electron transfers are concerted (the CPET pathway), the high-energy intermediates of the stepwise pathways are bypassed, although this thermodynamic benefit may have a kinetic cost. The primary task of kinetics-based mechanism analysis is therefore to distinguish the three pathways, quantifying the factors that govern the competition between them, which requires modeling of CPET reactivity. CPET models of varying sophistication have appeared, but the large number of parameters involved and the uncertainty of the quantum chemical calculations they may have to resort to make experimental confrontation and inspiration a necessary component of model testing and refinement.

Electrochemical PCETs are worthy of particular attention, if only because most applications in which PCET mechanisms are operative involve collection or injection of electricity through electrodes. More fundamentally, changing the electrode potential is an easy and continuous means of varying the driving force of the reaction, whereas the current flowing through the electrode is a straightforward measure of its rate. Consequently, the current–potential response in nondestructive techniques (such as cyclic voltammetry) can be read as an activation–driving force relationship, provided the contribution of diffusion has been taken into account. Intrinsic properties (properties at zero driving force) are consequently a natural outcome of the electrochemical approach.

In this Account, we begin by examining the modeling of CPET reactions and then describe illustrating experimental examples inspired by two biological systems, photosystem II and superoxide dismutase. One series of studies examined the oxidation of phenols with, as proton acceptor, either an attached nitrogen base or water (in water as solvent). Another addressed interconversion of aquo-hydroxo-oxo couples of transition metal complexes, using osmium complexes as prototypes. Finally, the reduction of superoxide ion, which is closely related to its dismutation, allowed the observation and rationalization of the remarkable properties of water as a proton donor. Water is also an exceptional proton acceptor in the oxidation of phenols, requiring very small reorganization energies, both in the electrochemical and homogeneous cases. These varied examples reveal general features of PCET reactions that may serve as guidelines for future studies, suggesting that research emphasis might be profitably directed toward new biological systems on the one hand and on the role of hydrogen bonding and hydrogen-bonded environments (such as water or proteins) on the other.

Published on the Web 03/16/2010 www.pubs.acs.org/acr
10.1021/ar9002812

Introduction

Starting from the conspectus proton-coupled electron transfers (PCET) reaction scheme, one of the main tasks of the kinetics-based mechanism analysis is to distinguish the three pathways one from the other. Another consists of uncovering the factors that govern the competition between these pathways. Systematic and successful mechanism analysis of electrochemical PCET reactions is quite recent, starting in 2004−2005.[1] It implied modeling of the kinetic reactivity of concerted (CPET) reactions.[2,3] This is the object of the first section of this Account.

In the examples of application of mechanism analysis inspired by photosystem II,[4] we refer both to oxidation of phenols as mimicking the oxidation of a tyrosine located in the proximity of a histidine serving as proton acceptor and to the way in which the oxygen evolution manganese cluster is able to catalyze the oxidation of water. This is also the case for artificial catalytic systems of the same reaction based on transition metal complexes[5] where the role of the metal(II)aquo-metal(III)hydroxo-metal(IV)oxo PCET sequence is deemed essential.

As concerns the second example, superoxide dismutases[6] catalyze the reaction:

$$2O_2^{\bullet -} + 2H^+ \rightarrow O_2 + H_2O_2$$

which may be decomposed in two half-reactions

$$O_2^{\bullet -} - e^- \rightleftarrows O_2$$

$$O_2^{\bullet -} + e^- + H^+ \rightleftarrows O_2H^-$$

$$O_2H^- + H^+ \rightleftarrows H_2O_2$$

The first half-reaction is a straightforward outersphere electron transfer, and the second is a typical proton-coupled electron transfer followed by a second proton uptake. The characteristics of the electrochemical reduction of $O_2^{\bullet -}$ in an aprotic solvent and its evolution upon addition of a weak acid such as water may thus provide insights into the mechanism of the dismutation reaction.

Water was also found to be a remarkable proton acceptor in the oxidation of phenols as resulted from a cyclic voltammetric investigation of the electrochemical oxidation of two phenols, 2,4,6-tri-*tert*-butyl phenol and phenol itself in the absence of buffers. The very small reorganization energies found called for a comparison with the homogeneous oxidation of phenol investigated by means of the flash photolysis and stopped-flow techniques.

Most of the results discussed below were gathered by means of cyclic voltammetry, which consists of monitoring the current resulting from isosceles triangular scanning of the electrode potential. Mechanism analysis is based on the shape, height, and potential location of the resulting current−potential responses and their variation with parameters such as scan rate and reactant concentrations (for an introduction to this technique, see ref 7).

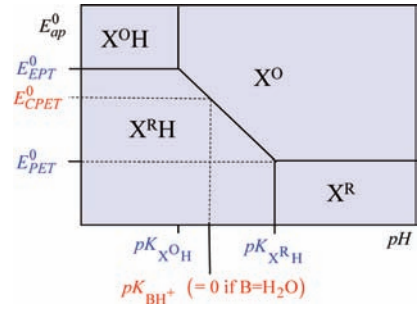

FIGURE 1. Pourbaix diagram showing the zones of thermodynamic stability of the various reactants in water.

Modeling Electrochemical CPET

The standard free energy of an electrochemical reaction (the opposite of the driving force) is given by $-F(E - E^0)$ for oxidation, where E is the electrode potential and E^0 is the standard potential of the redox couple (F is the Faraday constant). Each of the pathways in the conspectus scheme is characterized by a different E^0, defined from the standard chemical potentials (μ^0) as

$$E^0_{EPT} = \mu^0_{X^OH\cdots B} - \mu^0_{X^RH\cdots B}$$
$$E^0_{PET} = \mu^0_{X^O\cdots HB^+} - \mu^0_{X^R\cdots HB^+}$$
$$E^0_{CPET} = \mu^0_{X^O\cdots HB^+} - \mu^0_{X^RH\cdots B}$$

If the interaction represented by the H-bonds may be neglected, these standard potentials may be spotted on a Pourbaix diagram that relates the apparent standard potential, E^0_{ap}, to pH as shown in Figure 1, with E^0_{ap} being defined through the Nernst law describing the PCET thermodynamics:

$$E = E^0_{ap} + \frac{RT}{F}\ln\left(\frac{[X^O] + [X^OH]}{[X^R] + [X^RH]}\right)$$

The driving force of a CPET reaction where the proton is hosted in the HB^+/B couple is thus given by the value of E^0_{ap} for a pH equal to the pK of this acid−base couple. If the proton acceptor is water itself, the driving force corresponds to pH = 0, even if the pH of the experiment is different from 0, provided the solution does not contain other bases able to serve as proton acceptor in other CPET reactions.[8]

Rate laws in electrochemistry relate the current density, I, to the reductant and oxidant reactant concentrations *at the electrode surface*. The driving force of the reaction is involved

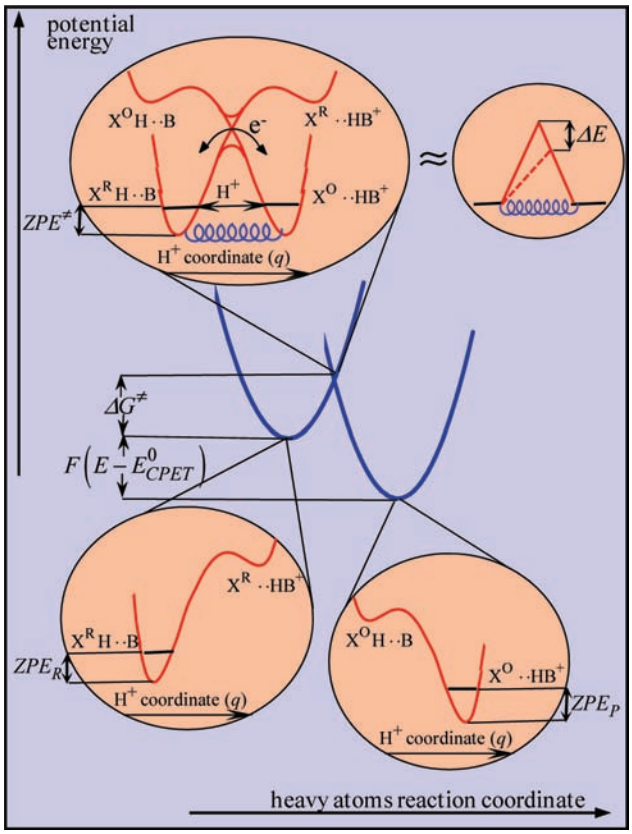

FIGURE 2. CPET: schematic representation of the potential energy profiles.

in the oxidation and reduction steps, with their ratio being given by the electrochemical oxidation equilibrium constant, $\exp[(F/RT)(E - E^0)]$. In most practical cases, this rate-driving force relationship, as applied to CPET reactions as well as to the electron-transfer steps in the stepwise pathways, may be linearized, giving rise to the so-called Butler−Volmer relationship:[2]

$$\frac{I}{F} = k_S^{ap} \exp\left[\frac{\alpha F}{RT}(E - E^0)\right]\left\{[\text{red}] - \exp\left[-\frac{F}{RT}(E - E^0)\right][\text{ox}]\right\} \quad (1)$$

with

$$k_S^{ap} = k_S \exp\left[-(\alpha + z_R)\frac{F\phi_S}{RT}\right]$$

(k_S, k_S^{ap} = true and apparent standard rate constants, α = transfer coefficient, z_R = reactant charge, ϕ_S = potential difference between the reaction site and the solution). Application of eq 1 to electron transfers in the stepwise pathways is justified by the fact that they are outersphere electron transfers and that the value of the transfer coefficient, α, may be considered as constant (but not necessarily equal to 0.5) over the relatively narrow potential excursion in standard cyclic voltammetric experiments. But what about the applicability of these relationship for CPET reactions? A simplified model was developed[2] based on the ideas detailed in ref 9 for proton transfer. The four diabatic states represented in Figure 2 are mixed to generate two states that are adiabatic toward proton transfer, as shown in the upper inset. Both electron and proton being light particles as compared to the other atoms, their transfer requires, according to the Born−Oppenheimer approximation, reorganizing the heavy atoms, including those of the solvent to reach a transition state where both reactants and products have the same configuration. The electron being much lighter than the proton, a second application of the Born−Oppenheimer approximation entails that the electron is transferred at the avoided crossing intersection of the potential energy profiles of the resulting two states while the proton tunnels through the barrier thus formed (Figure 2). Figure 2 exemplifies a proton transfer occurring between two proton vibrational ground states. Proton excited states may be additionally involved but usually to a lesser extent.[2b] In the rate law relating the current density to the electrode potential,

$$\frac{I}{F} = k(E)\left\{[\text{red}] - \exp\left[-\frac{F}{RT}(E - E^0)\right][\text{ox}]\right\}$$

the potential-dependent rate constant, $k(E)$, may be expressed, as the product of a pre-exponential factor, Z, by the classical quadratic Marcus−Hush term related to the harmonic approximation sketched in Figure 1:

$$k(E) = Z \exp\left[-\frac{\lambda}{4RT}\left(1 - F\frac{E - E^0}{\lambda}\right)^2 - \frac{\Delta\text{ZPE}}{RT}\right]$$

where λ is the reorganization energy of the heavy atoms during the reaction. $\Delta\text{ZPE} = \text{ZPE}^{\neq} - \text{ZPE}_R$ is the difference between the transferring proton zero-point energies at the transition state and at the reactant state. The pre-exponential factor $Z = Z^{el}\chi$ is the product of the collision frequency $Z^{el} = (RT/2\pi M)^{1/2}$ (M = reactant molar mass) by the transmission coefficient $\chi = 2p/(1 + p)$, where p is the probability of proton tunneling and electron transfer, which occurs at the transition state as sketched in the upper inset of Figure 2. p is obtained from the Landau−Zener relationship:

$$p = 1 - \exp\left[-\pi\left(\frac{C}{RT}\right)^2\sqrt{\frac{\pi RT}{\lambda}}\right]$$

in which C is the coupling energy between the reactant and product proton vibrational states at the transition state, obtained semiclassically from the ground state profile, $V(q, Q)$

$$C(Q) = h\nu_0^{\neq} \exp\left[-2\pi/h\left(\int_{q_i}^{q_f}\sqrt{2m_P(V(q, Q) - E)}\,dq\right)\right]$$

where Q is the distance between the donor and acceptor atoms, q is the proton coordinate, $\nu_0^{\neq}$ is the proton well fre-

quency, m_P is the proton mass, and q_i and q_f are the classical turning points in each well at fixed Q. It follows that χ is a function of Q to be averaged according to $\chi = \int_{-\infty}^{+\infty} \chi(Q)\, P(Q)\, dQ$ over the Boltzmann distribution (as recalled by the blue spring in the upper insets of Figure 2), which emphasizes the importance of small values of Q in proton tunneling.

So far, only Fermi-level electronic states of the electron in the electrode have been taken into account. Taking into account all electronic states of the electrons in the electrode leads to a somewhat cumbersome expression of the overall rate law. However, considering the fact that the potential excursion in a cyclic voltammetric experiments does not exceed a few hundred millivolts, the rate law may be linearized leading to the applicability of rate law (1) and to the following expression of the apparent standard rate constant:[2]

$$\ln\left(\frac{k_S^{ap}}{T}\right) = \ln\left(\frac{\chi R}{2\sqrt{2M\lambda}}\right) - \frac{\lambda/4 + (\alpha + z_R)F\phi_S + \Delta ZPE}{RT} \quad (2)$$

which can be read as an Arrhenius plot, the slope and intercept of which provide an estimation of the reorganization energy and of the transmission coefficient, respectively, to be compared to the predictions of the model.

We note en passant that a Marcus-type inverted region is not expected in CPET reactions for two reasons: contribution of electrode electronic states outside of the Fermi level and contribution of proton excited states.[3,9]

The reorganization energy λ is the sum of an intramolecular contribution, λ_i, and a solvent reorganization energy, λ_0. λ_i may be estimated quantum-mechanically by calculating the energy of the product system in the configuration of the reactant system or vice versa. λ_0 is itself the sum of two contributions according to an electrostatic model developed in ref 2a:

$$\lambda_0^{ET} = \frac{e^2}{4\pi\varepsilon_0}\left(\frac{1}{\varepsilon_{op}} - \frac{1}{\varepsilon_S}\right)\frac{1}{2a} \quad (3)$$

and

$$\lambda_0^{PT} = \frac{1}{4\pi\varepsilon_0}\left(\frac{\varepsilon_S - 1}{2\varepsilon_S + 1} - \frac{\varepsilon_{op} - 1}{2\varepsilon_{op} + 1}\right)\frac{(\mu_R - \mu_P)^2}{a^3} \quad (4)$$

(ε_0 = vacuum permeability, ε_{op}, ε_S = optical and static dielectric constants of the solvent, respectively, a = radius of the reactant equivalent sphere, and μ_R, μ_P = dipole moments of the reactant and product, respectively). The first contribution is usually much larger than the second. They are typically in the ratio 90:10 (see next section).

The estimation of χ using the above series of equations is simplified by means of the isosceles triangle approximation of the proton-tunneling barrier shown in the upper-right inset of Figure 2.[2b] Note that the vicinity of the electrode may produce an electric field effect, symbolized by ΔE and the dashed line in the upper-right insert of Figure 2, which decreases the height and the thickness of the proton-tunneling barrier, resulting in an increased degree of adiabaticity (see an illustration of this effect in the next section).

The CPET pathway is expected to be endowed with a H/D kinetic isotope effect, which may be used as a diagnostic criterion in mechanism discrimination as developed in the next sections. In the framework of the CPET pathway, since the reorganization energy and the double-layer correction are expected to be practically the same in both cases, $k_{S,H}^{ap}/k_{S,D}^{ap}$ depends essentially on the variation in zero-point energies and on the tunneling of proton (viz. deuteron) represented by the values of the transmission coefficient:

$$\frac{k_{S,H}^{ap}}{k_{S,D}^{ap}} = \frac{\chi_H}{\chi_D}\exp\left[\frac{-\Delta ZPE_H + \Delta ZPE_D}{RT}\right]$$

For adiabatic CPETs, that is, for $\chi = 1$, typical values are of the order of 1.5, whereas larger values are observed when the degree of nonadiabaticity increases (see next sections).

Oxidation of Phenols with an Attached Proton Acceptor

Oxidation of phenols is facilitated by the presence of a proton accepting group such as an amine, forming a H-bond in structures such as that shown in Figure 3, mimicking the tyrosine$_Z$-histidine 190 pair in photosystem II. Cyclic voltammetry in an aprotic solvent (Figure 3) shows a reversible wave corresponding to the one-electron−one-proton reversible conversion from phenol + amine to the phenoxyl radical + ammonium ion, which may take the pathways shown in the conspectus scheme.[10] That the CPET pathway prevails results from the simulations shown in Figure 3a of the cyclic voltammetric responses corresponding to the stepwise pathways. Using values bracketing the standard potentials and equilibrium constants of each step of the stepwise pathways clearly shows complete disagreement with the low-scan rate response (Figure 3a). The CPET kinetics interferes upon raising the scan rate, revealing a small ($k_{S,H}^{ap}/k_{S,D}^{ap} = 1.6$) but definite H/D kinetic isotope effect (Figure 3b), in line with the CPET mechanism. Estimation of the degree of adiabaticity and reorganization energy may be obtained from the application of eq 2 to the Arrhenius plot shown in Figure 3c. It thus appears that $\chi = 1$ and

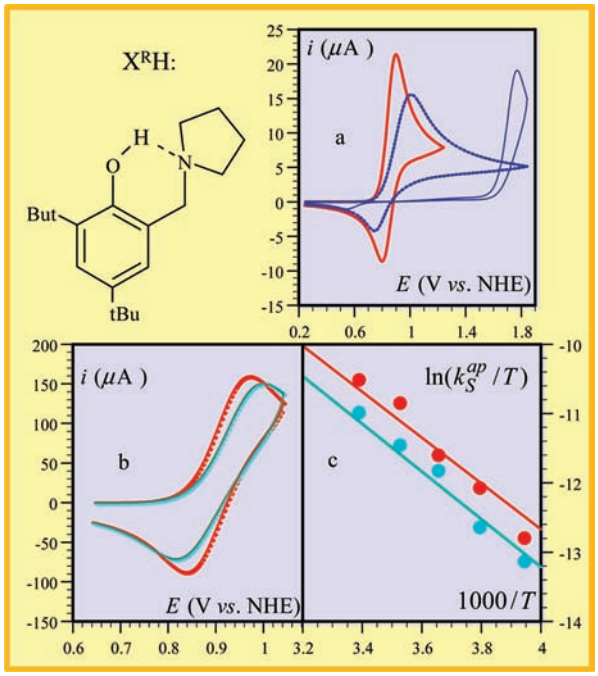

FIGURE 3. Cyclic voltammetry in acetonitrile of the aminophenol shown. (a) Red, experimental trace at 0.2 V/s; blue, simulation of the stepwise pathways. (b) H/D kinetic isotope effect. Cyclic voltammetry at 0.5 V/s in the presence of 2% CH_3OH (red) and CD_3OD (cyan). (c) Arrhenius plots in the presence of 2% CH_3OH (red) and CD_3OD (cyan).

$$\frac{\lambda}{4} + \alpha F\phi_S + \Delta ZPE = 0.285 \text{ eV (for H)}, 0.297 \text{ eV (for D)}$$

Since the cyclic voltammetric response is close to reversible, $\alpha \simeq 0.5$. Using $k^{ap}_{S,H}/k^{ap}_{S,D} = \exp[(\Delta ZPE_H/RT)(1/\sqrt{2} - 1)] = 1.6$, ΔZPE_H can be estimated as equal to -0.04 eV and thus $\lambda = 1.06$ eV.[2b] This rather modest value of the reorganization energy may be rationalized using eqs 3 and 4, which leads, with literature or estimated values of the various parameters, to $\lambda_0^{ET} = 0.713$ eV, $\lambda_0^{PT} = 0.062$ eV, $\lambda_i = 0.375$ eV, and thus $\lambda = 1.15$ eV,[2b] in good agreement with the experimental value. The agreement is far from being as good concerning the transmission coefficient. Indeed, application of the preceding triangle model leads to $\chi = 0.004$, instead of 1. This discrepancy has been suggested to result from an electric field effect due to the reactant site being located close to the electrode surface within the strong double layer electric field, corroborated by a quantitative estimate of this effect.[2b]

It is interesting to compare these electrochemical results to the oxidation of similar amino phenols by homogeneous reactants.[11] Arrhenius plots obtained for the reaction shown in Scheme 1[11] may be analyzed by means of a homogeneous version of eq 2:[2b−c]

$$\ln\left(\frac{k}{\sqrt{T}}\right) = \ln\left(N_A\chi d^2\sqrt{\frac{8\pi R}{M}}\right) + \frac{\Delta S^0}{2R} - \frac{\frac{\lambda}{4} + \frac{\Delta H^0}{2} + \Delta ZPE}{RT}$$

(M = molar mass, d = distance between the centers of the reactant equivalent spheres, ΔH^0 and ΔS^0 = standard enthalpy and entropy of the reaction, respectively) from which the reorganization energy, λ, and the transmission coefficient, χ, can be derived taking for ΔH^0 and ΔS^0 the values obtained from the variation with temperature of the difference in standard potentials between the CPET and $ArN^{\bullet+}$/ArN redox couple. The reaction appears as nonadiabatic ($\chi \simeq 0.01$), in line with theoretical estimates, in contrast with the electrochemical counterpart owing to the electric field effect discussed earlier. This is the main difference between the two types of reactions. The value of the reorganization energy, 0.8 eV, is consistent with what was found in the electrochemical case, provided ΔH^0 and ΔS^0 are taken into account[2b] (if not, improperly large values are found[11]).

Amine groups attached to the phenol structure are not the only efficient proton acceptors. Carboxylate groups, also frequent in natural systems, play a similar role as illustrated by the example depicted in Scheme 2 where the ortho, ortho′-dicarboxylato-hydrobenzoquinone is electrochemically oxidized with concomitant transfer of the proton to the carboxylate.[12] A CPET pathway is also taken for the further oxidation generating benzoquinone with proton transfer to the second carboxylate.

Oxidation of Phenols in Water with Water as the Proton Acceptor

Water is an ubiquitous solvent in natural and industrial processes where it can also act as proton donor and acceptor. Its role in PCET reactions as a peculiar, H-bonded and H-bonding medium is obviously of considerable interest. Although investigated over decades, the mechanisms of proton conduction in water are still under active experimental and theoretical scrutiny.[13] The mechanism of PCET reactions involving water should deserve the same attention. Oxidation of phenols in unbuffered water recently offered the opportunity of a detailed characterization of PCET s in water. Investigation of

SCHEME 1

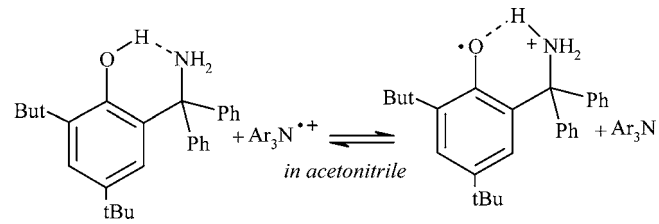

SCHEME 2

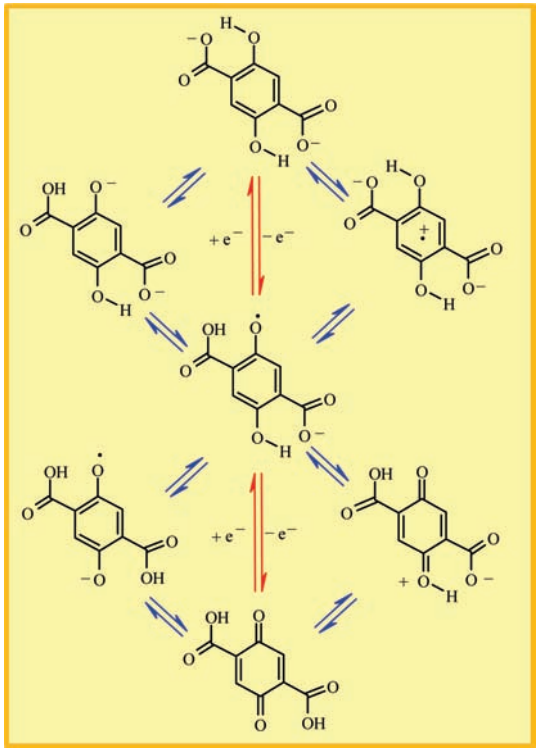

the electrochemical oxidation of tri-*t*-butylphenol as a function of pH showed that the competition between a OH^--PET pathway and a H_2O-CPET pathway could be read directly on the cyclic voltammetric responses.[14] Thanks to steric hindrance to dimerization of the phenoxyl radicals brought about by the *t*-butyl groups, two reversible waves, each of them corresponding to one mechanism, are observed. This advantageous feature is however counterbalanced by the necessity of using a 1−1 water−ethanol solvent, for solubility reasons, which hampers a full quantitative characterization of the reaction. This drawback is not met with phenol (PhOH) itself, and the mechanism, even if somewhat more complicated by phenol dimerization, may well be teased out provided this additional reaction is properly taken into account (in the conspectus scheme, now: X^RH = PhOH, B = OH^-, H_2O).[15] The thermodynamics of the reaction was determined in buffered water taking into account the kinetics of the dimerization reaction according to the procedure summarized in Figure 4a−c, leading to the values of all characteristic pK's and standard potentials in Figure 4c.

In unbuffered water (Figure 4d,e), starting from basic media, the oxidation wave splits in two waves as the pH decreases, showing peak potential variations that are strikingly different from those obtained in buffered media. The first wave stands for an OH^--PET pathway controlled by the diffusion of OH^- ions toward the electrode,[15] and the second wave for an EPT or a H_2O−CPET pathway. The first possibility is ruled out by kinetic analysis and simulation (blue line in Figure 4e)[15] and observation of a small but definite H/D kinetic isotope effect (2.5). Analysis of the CPET reaction according to eqs 1 and 2 leads to $k_S^{H_2O\text{-}CPET} = 25$ cm s^{-1} and $\lambda_{CPET} = 0.4$ eV. Reaching such a high standard rate constant (the highest ever measured by means of cyclic voltammetry) was made possible by the partial kinetic control by proton diffusion resulting from the use of an unbuffered medium.[15] Also striking is the smallness of the reorganization energy. In this connection, it is interesting to see whether this feature also transpires in homogeneous oxidation of phenol in neat water. The results of a recent photochemical and stopped-flow study of this question are summarized in Figure 5.[16] Variation of the overall rate constant, k_+, with pH showed the transition between a direct

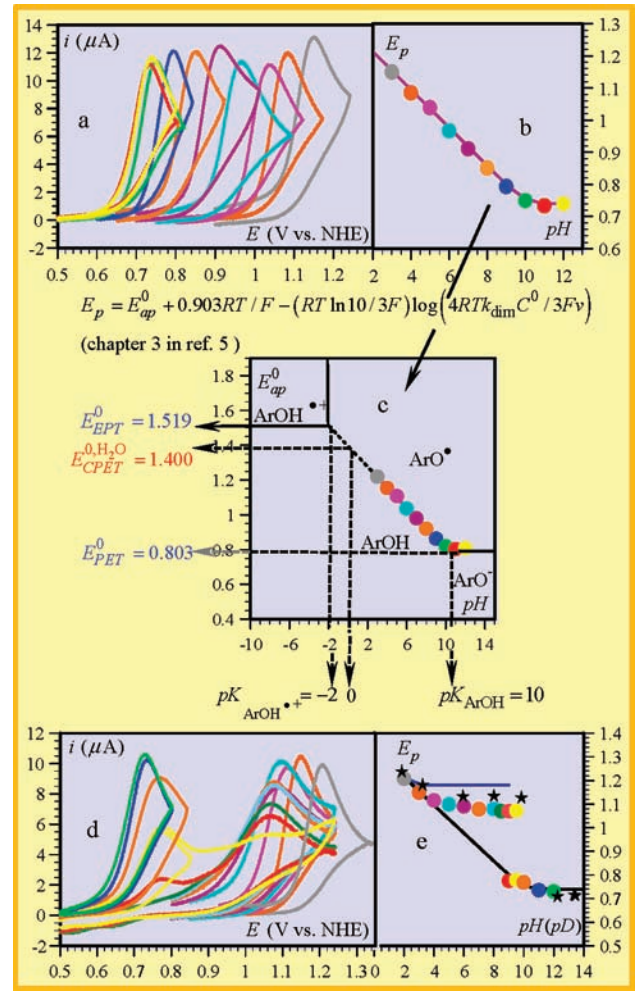

FIGURE 4. Cyclic voltammetry of phenol (PhOH) in water at 0.2 V/s. (a−c) In 0.1 M Britton−Robinson buffers (potentials in V vs. NHE); (d,e) in unbuffered water. The black stars are the peak potentials in D_2O, and the upper blue line is the simulated variation of the peak potential for an EPT mechanism. The color code of the voltammograms and the peak potentials are the same.

phenol oxidation reaction at low pH, where the rate constant, k_1, does not vary with pH and an OH^--PET pathway with a rate constant k_2:

$$k_+ = \frac{[ArOH]}{[ArOH]_{total}} k_1 + \frac{[ArO^-]}{[ArOH]_{total}} k_2 \qquad (5)$$

The transition between phenol and phenoxide ion oxidation is characterized by a unity-slope variation. In no case did these data show the 1/2 slope previously reported for the oxidation of phenol by $Ru^{III}(bpy)_3$.[17] The latter behavior was explained by means of the incorrect[18,8] notion of pH-dependent driving force. In water, with no other proton acceptor present, water and the proton produced upon oxidation are reactants in the CPET process. The driving force is therefore governed by the standard potential of this reaction, $FE^0_{CPET} = \mu^0_{H_3O^+} + \mu^0_{ArO^\bullet} - \mu^0_{ArOH} - \mu^0_{H_2O}$ (μ^0 = the *standard* chemical potentials), which does not depend on pH. It is equal to the apparent standard potential at pH = 0. Consequently, the 1/2-slope variation with pH sometimes reported may not be taken as a diagnostic criterion of the occurrence of a CPET mechanism. Derivation of the characteristics of counter-diffusion

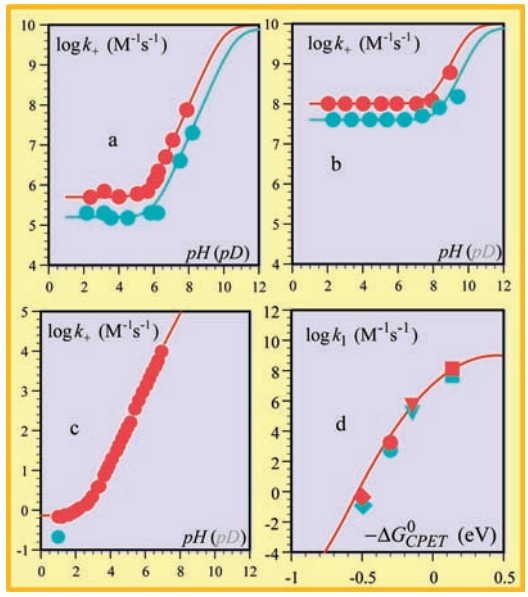

FIGURE 5. Variation with pH (or pD) of the overall forward rate constant of phenol + phenoxide oxidation by the various electron acceptors. (a) $Ru^{III}(bpy)_3$, (b) $Ru^{III}(4,4'\text{-}CO_2Et\text{-}bpy)_2(bpy)$, (c) $Ir^{IV}Cl_6$. Red dots: results obtained in H_2O by the laser flash technique in (a) and (b) and by the stopped-flow method in (c).[19] Cyan dots: results obtained in the same way in D_2O. Red and cyan lines: application of eq 5 to the H_2O and D_2O data, respectively. (d) Forward rate constant of phenol oxidation by the various electron acceptors. Red and cyan symbols: H_2O and D_2O, respectively; squares: $Ru^{III}(bpy)(4,4'\text{-}CO_2Et\text{-}bpy)_2$, triangles: $Ru^{III}(bpy)_3$; circles: $Ru^{III}(4,4'\text{-methyl-bpy})_3$ (k_1 determined at pH = 3); tilted squares: $Ir^{IV}Cl_6$. Red line: activation-controlled rate constant predicted for a pre-exponential factor of 2×10^9 $M^{-1}s^{-1}$ and a reorganization energy of 0.5 eV.

intermolecular reactions allowed showing that the concerted process is under activation control. It is characterized by a remarkably small reorganization energy (0.5 eV), in line with what was determined in the electrochemical case. It is interesting to note that these reorganization energies are much smaller than those for the outersphere oxidation of phenoxide ions in the same conditions, 0.80 and 1.27 eV in the electrochemical and homogeneous case, respectively.[16] The remarkably small values of the CPET reorganization energies underpin the very peculiar behavior of water as proton acceptor when it is used as the solvent.

Aquo-Hydroxo-Oxo Couples of Transition Metal Complexes: The Example of Osmium Complexes

The electrochemical oxidation of the $X^RH = [bpy_2pyOs^{II}\text{—}OH_2]^{2+}$ (py, pyridine; bpy, 2,2′-bispyridine) complex in water has recently been taken as an illustrative example in the quest of concerted pathways in metal(II)aquo-metal(III)hydroxo-metal(IV)oxo PCET sequences.[20] The two successive waves (Figure 6a) correspond to the passage in the conspectus scheme, successively, from $Os^{II}\text{—}OH_2$ (X^RH) to $Os^{III}\text{—}OH$ (X^O) and from $Os^{III}\text{—}OH$ (X^RH) to $Os^{IV}\text{—}O$ (X^O). The variation of the apparent standard potential, E^0_{ap}, obtained as the midpoint of each pair of peaks, with pH, defines the zones of thermodynamic stability of the various intervening species (Figure 6b). It immediately appears, from the peak separations, that the first couple is much faster than the second and therefore requires using a higher scan rate for a kinetic characterization. The apparent standard rate constant, k_S^{ap}, was obtained from the application of the Butler—Volmer approximation with $\alpha = 0.5$ (the overpotential is small in all cases). It follows that, assuming, as seems likely, that all protonation/deprotonation steps are so fast as to be under unconditional equilibrium:

$$\frac{i}{FSC^0} = k_S^{ap} \exp\left[\frac{F}{2RT}\left(E - E^0_{ap}\right)\right] \left(\frac{\sum^{II \text{ or } III}}{C^0} - \frac{\sum^{III \text{ or } IV}}{C^0} \exp\left[-\frac{F}{RT}\left(E - E^0_{ap}\right)\right]\right)$$

with:

$$k^{ap}_{S,III/II \text{ or } IV/III} = k^{CPET}_{S,\text{ or } IV/III}\sqrt{[B][HB^+]} + k^{EPT}_{S,III/II \text{ or } IV/III}\sqrt{\frac{[H^+]}{K_{Os^{III}OH_2 \text{ or } Os^{IV}OH}}} + k^{PET}_{S,III/II \text{ or } IV/III}\sqrt{\frac{K_{Os^{II}OH_2 \text{ or } Os^{III}OH}}{[H^+]}}$$

Fitting of experimental data in H_2O and D_2O (Figure 6c) with these equations shows that the stepwise pathways predominate

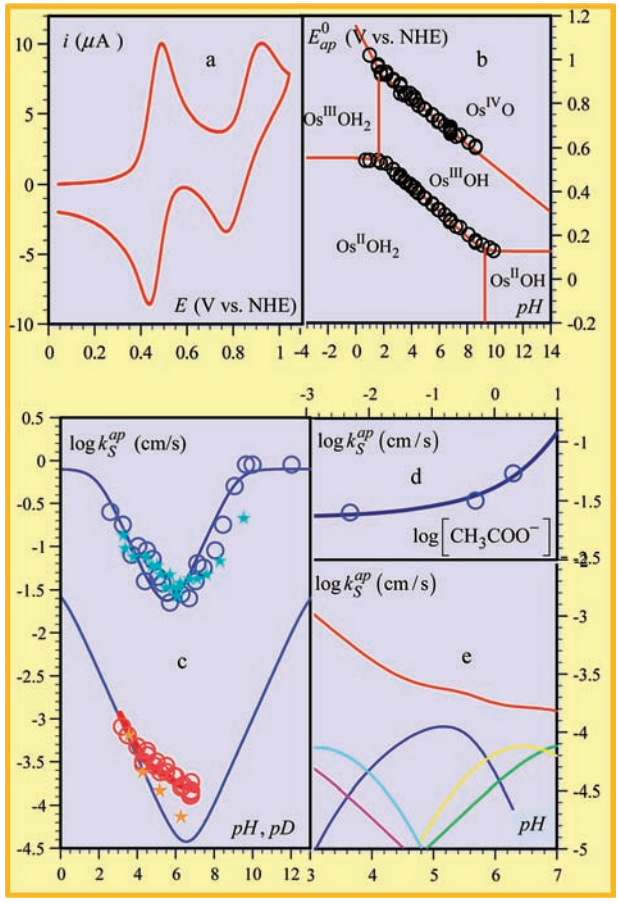

FIGURE 6. Cyclic voltammetry of $[bpy_2pyOs^{II}-OH_2]^{2+}$ in a 0.1 M Britton−Robinson buffer. (a) Typical two-wave 0.2 V/s voltammogram at pH = 3. (b) Variation of the apparent standard potential with pH. (c) Variation with pH of the apparent standard rate constant of the Os^{II}/Os^{III} (H_2O, blue circles; D_2O, cyan stars) and Os^{III}/Os^{IV} couples (H_2O, red circles; D_2O, orange stars). Blue lines: prediction for stepwise mechanisms with the two couples. Red line: prediction for a CPET mechanism with the Os^{III}/Os^{IV} couple. (d) Dependence of the apparent standard rate constant of the Os^{II}/Os^{III} couple on buffer concentration in an aqueous acetate buffer at pH 5. (e) Contribution of each buffer couple to the Os^{III}/Os^{IV} CPET reaction. Magenta and green: phosphoric acid, pK = 2.16 and 7.21, respectively. Cyan, blue, and yellow: citric acid, pK = 3.15, 4.77, and 6.40, respectively.

with the Os^{II}/Os^{III} couple, whereas the concerted pathway prevails with the Os^{III}/Os^{IV} couple. For the first couple, very large amounts of the buffer have to be added to trigger the CPET pathway (Figure 6d). This finding provided an interpretation[20a] of the observation of a CPET mechanism with a similar osmium complex assembled on a gold electrode[21] together with carboxylate groups serving as proton acceptors. As to the Os^{III}/Os^{IV} couple, the contributions of the various bases contained in the buffer are detailed in Figure 6e.

This mechanistic analysis is not only the first that rigorously discriminates between stepwise and concerted pathways in PCET reactions involving the coordination sphere of transition metal complexes, but it also nicely illustrates the notion that CPET pathways, in contrast with stepwise pathways, allow avoidance of high-energy intermediates: in the first couple, in which the stepwise pathways predominate, the intermediates are formed at pH's well inside the accessible domain; in the second, in which the concerted pathway prevails, they stand clearly out of the accessible pH range.

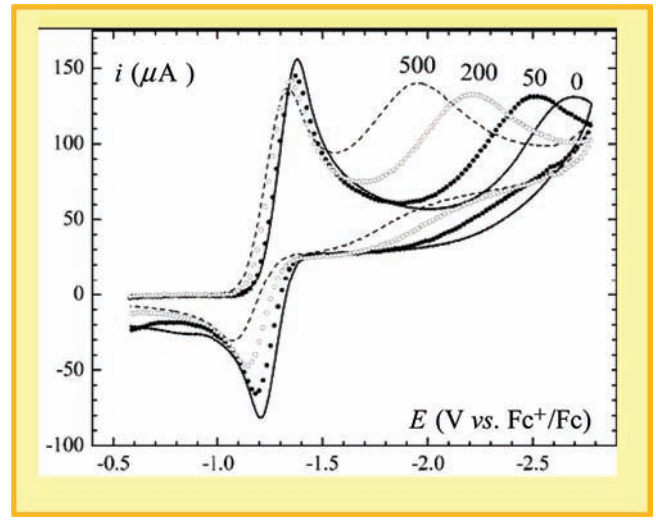

FIGURE 7. Cyclic voltammetry of the reduction of dioxygen in acetonitrile (+ 0.1 M NBu_4PF_6) at a glassy carbon electrode at 0.50 V/s in the presence of increasing H_2O concentrations (numbers on each curve in mM).[22b] Add 0.645 V to obtain a potential scale referred to the NHE.

Reduction of Superoxide Ion

The reduction of $O_2^{\bullet-}$ (our only example of reductive CPET) is another case where water, used this time as proton donor, displays remarkable traits. It was also the first electrochemical example where the occurrence of a CPET mechanism was firmly established.[22] In an aprotic solvent, dioxygen shows an almost reversible cyclic voltammetric first wave (Figure 7). The second thick and irreversible wave corresponds to the reduction of the superoxide ion produced at the first wave. It is heavily dependent on the concentration of water, suggesting the CPET pathway depicted in Scheme 3. In addition to the CPET mechanism, the PET mechanism is also acting, but at the level of the first wave rather than at the second wave. The slight irreversibility of the first wave and its electron stoichiometry, a little larger than one, indicate that the superoxide ion is protonated to a small extent and the resulting $HO_2^{\bullet}$ radical is immediately reduced at the electrode or in solution by another superoxide ion along an "ECE-DISP" mechanism.[7] At the second wave, the CPET route is followed rather than the EPT route, as attested by a small but significant H/D isotope effect (= 2).

SCHEME 3

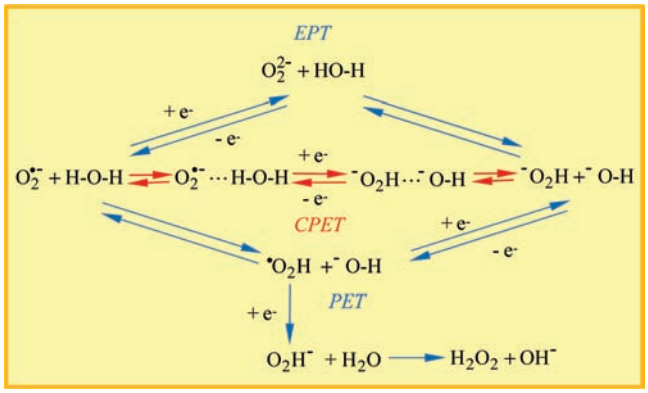

SCHEME 4

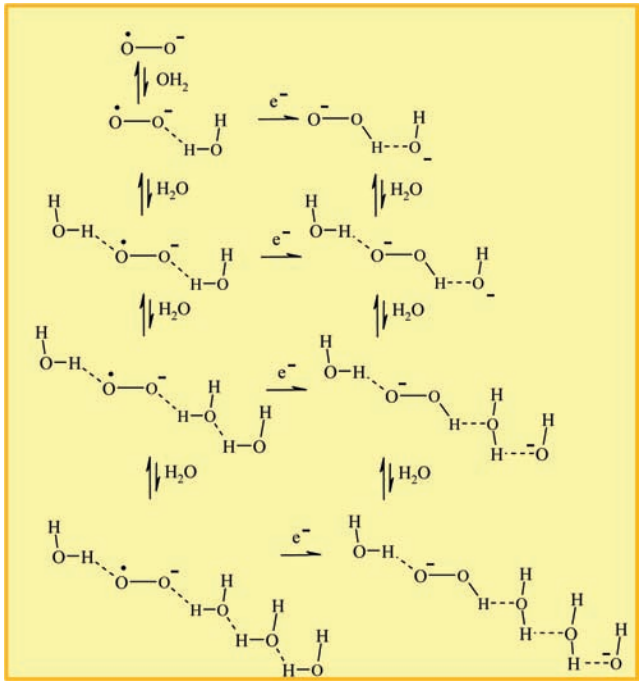

The CPET reduction of $O_2^{\bullet-}$ exhibits a huge variation of the peak potential with water concentration (Figure 7), paralleled by an increase of the H/D isotope effect. The standard potential, $E^0_{O_2^{\bullet-}+H_2O/O_2H^-+OH-}$, derived from the second wave is an increasing function of the water concentration, which variation reveals the formation of 1−1 and 1−2 $O_2^{\bullet-}$−H_2O adducts. The one-electron transfer product (a set of two negative ions, HO_2^- and OH^-) is sensitive to this specific solvation to an even larger extent. A positive shift of the standard potential, and consequently of the peak potential, is thus expected. However, unrealistically small values of the peak shifts are thus anticipated, suggesting instead the mechanism sketched in Scheme 4:[23] a concerted transfer of one electron and one proton through short water chains is favored thermodynamically by a decrease of the attending repulsion between HO_2^- and OH^- even though there is some kinetic counterpart to this advantage, falling in line with the increase of the H/D kinetic effect with concentration, reflecting the increase in the H^+ tunneling distance. The reduction of benzophenone anion radical in an aprotic solvent shows a remarkably similar behavior upon addition of water.[24]

Conclusions and Prospects

Examples of electrochemical PCET reactions as diverse as oxidation of phenols, oxido-reductive conversion in a metal-aquo/hydroxo/oxo sequence and reduction of superoxide ion have been successfully analyzed in terms of mechanism by means of a nondestructive technique, namely, cyclic voltammetry. The outcome is an increased knowledge not only on these particular systems but also on the classes of reactions they illustrate as typical examples.

On the methodological side, these analyses constitute a test of procedures that can now be applied to any other system. The main advantage of the electrochemical approach is that changing the electrode potential is an easy way of varying the driving force of the reaction, as compared to homogeneous approaches, which would require the use of numerous electron donor or acceptor coreactants to the substrate of interest to span an equivalent range of driving forces. Consequently, electrochemistry offers an easier access to standard rate constants (rate constant at zero driving force) than do the other approaches. The main drawback of the electrochemical approach is the necessity of constantly checking the surface conditions of the electrode in order to obtain reproducible results. Note however that other approaches such as the photochemical approach are not devoid of difficulties, particularly those related to spurious side-reactions that may perturb the overall kinetics (see, e.g., the oxidation of phenol by photogenerated ruthenium(III) complexes). These are the reasons that investigating the same reacting system by electrochemistry and by other approaches is worthwhile in most cases. For example, the extremely small intrinsic barrier for the oxidation of phenol with water (in water) as the proton acceptor found electrochemically was usefully confirmed by analysis of homogeneous oxidation of the same system. From the rather scarce available comparative data, it appears that proton tunneling is easier in the electrochemical case than in the homogeneous case, whereas intrinsic barriers are of the same order of magnitude.

Comprehension of the CPET reactions and of the factors that govern competition with stepwise pathways is in its infancy. Even in crude theoretical models, and a fortiori in more sophisticated ones, the number of parameters that

should be adjusted or derived from uncertain calculations is so large that a semiempirical approach remains necessary. Starting from pertinent experimental examples suggested by crude theoretical estimations and by past examples, one will try to uncover the most important reactivity factors so as to both simplify and improve the theoretical CPET models and systematize the parameters of the competition with stepwise pathways. Combination of electrochemical and other approaches applied to the same experimental systems appears as essential, with, in both cases, a particular effort directed toward the determination of the intrinsic CPET characteristics. We may then expect to progressively build reactivity−structure relationships that involve not only the molecule being oxidized or reduced but also the proton acceptor. In this respect, understanding the remarkably high reactivity of systems in which water (in water) is the proton acceptor deserves particular attention.

As progress is made in these fundamental matters, one may expect that increasingly complex systems, in which PCET reactions are key rate-controlling factors, will be amenable to mechanistic and reactivity analysis. One has naturally in mind the huge number of natural systems in which PCET reactions play a central role, but also catalytic devices, bioinspired or not, devised to confront modern energy challenges contain PCET reactions. Concerning electrochemical reactions, systems immobilized onto the electrode surface will certainly attract particular attention.

Julien Bonin, Cyril Louault, Mathilde Routier, and Anne-Lucie Teillout are thanked for their participation to the work described in this Account. Partial financial support from ANR PROTOCOLE is gratefully acknowledged.

Note Added after ASAP. This paper was published on March 16, 2010 with errors in the caption for Figure 7. The revised version was published on March 19, 2010.

BIOGRAPHICAL INFORMATION

Cyrille Costentin received his undergraduate education at Ecole Normale Supérieure in Cachan and pursued his graduate studies under the guidance of Profs. Jean-Michel Savéant and Philippe Hapiot at the University Paris Diderot (Paris 7), where he received his Ph.D. in 2000. After 1 year as a postdoctoral fellow at the University of Rochester, working with Prof. J. P. Dinnocenzo, he joined the faculty at the University of Paris Diderot as associate professor. He was promoted to professor in 2007. His interests include mechanisms and reactivity in electron transfer chemistry with particular recent emphasis on electrochemical and theoretical approaches to proton-coupled electron transfer processes.

Marc Robert was educated at the Ecole Normale Supérieure in Cachan, France and obtained his Ph.D. in 1995 at the Paris Diderot University (Paris 7) under the supervision of Claude P. Andrieux and Jean-Michel Savéant. After 1 year as a postdoctoral fellow at The Ohio State University, working alongside Matt Platz, he joined the faculty at Paris Diderot University as associate professor. He was promoted to professor in 2004 and has been a member of the University institute of France since 2007. His interests include electrochemical, photochemical, and theoretical approaches of electron transfer reactions, as well as proton-coupled electron transfer processes in both organic chemistry and biochemistry.

Jean-Michel Savéant received his education in the Ecole Normale Supérieure in Paris, where he became the Vice-Director of the Chemistry Department before moving to the University Paris Diderot (Paris 7) as a Professor in 1971. He is, since 1985, Directeur de Recherche au Centre National de la Recherche Scientifique in the same university. In 1988−1989, he was a visiting professor at the California Institute of Technology. His current research interests involve all aspects of molecular and biomolecular electrochemistry as well as mechanisms and reactivity in electron transfer chemistry and biochemistry. He is a Member of the French Academy of Sciences and a Foreign Associate of the National Academy of Sciences of the United States of America.

FOOTNOTES

*To whom correspondence should be addressed. E-mail: saveant@univ-paris-diderot.fr.

REFERENCES

1 (a) The notion of concerted proton-electron transfer is also recent.[1b] (b) Biczok, L.; Linschitz, H. Concerted Electron and Proton Movement in Quenching of Triplet C60 and Tetracene Fluorescence by Hydrogen-Bonded Phenol-Base Pairs. *J. Phys. Chem.* **1995**, *99*, 1843–1845. (c) There is unfortunately no consensus on definitions and acronyms. We use PCET (proton-coupled electron transfer) for all reactions in which, whatever the mechanism, reactant and product systems differ by the exchange of one electron and one proton. CPET is reserved for PCET reactions in which electron and proton transfers are concerted. The most perturbing aspect of this lack of agreement on nomenclature, which should particularly alert the reader, is that some authors use PCET or EPT to mean CPET. Much less serious is the replacement, in the designation of stepwise pathways, of EPT and PET by ETPT and PTET.

2 (a) Costentin, C.; Robert, M.; Savéant, J.-M. Electrochemical concerted proton and electron transfers. Potential-dependent rate constant, reorganization factors, proton tunneling and isotope effects. *J. Electroanal. Chem.* **2006**, *588*, 197–206. (b) Costentin, C.; Robert, M.; Savéant, J. M. Adiabatic and Non-adiabatic Concerted Proton-Electron Transfers. Temperature Effects in the Oxidation of Intramolecularly Hydrogen-Bonded Phenols. *J. Am. Chem. Soc.* **2007**, *129*, 9953–9963. (c) Costentin, C.; Robert, M.; Savéant, J. M. Adiabatic and Non-adiabatic Concerted Proton-Electron Transfers. Temperature Effects in the Oxidation of Intramolecularly Hydrogen-Bonded Phenols. *J. Am. Chem. Soc.* **2010**, *132*, 2845 (correction).

3 Hammes-Schiffer, S. Theory of Proton-Coupled Electron Transfer in Energy Conversion Processes. *Acc. Chem. Res.* **2009**, *42*, 1881–1889.

4 Rutherford, A. W.; Boussac, A. Biochemistry: Water Photolysis in Biology. *Science* **2004**, *303*, 1782–1784.

5 Savéant, J.-M. Molecular Catalysis of Electrochemical Reactions. Mechanistic Aspects. *Chem. Rev.* **2008**, *108*, 2348–2378.

6 Miller, A.-F.; Padmakumar, K.; Sorkin, D. L.; Karapetian, A.; Vance, C. K. Proton-coupled electron transfer in Fe-superoxide dismutase and Mn-superoxide dismutase. *J. Inorg. Biochem.* **2003**, *93*, 71–83.

7 Savéant, J.-M. *Elements of Molecular and Biomolecular Electrochemistry*; Wiley-Interscience: New York, 2006.

8 Costentin, C.; Robert, M.; Saveant, J. M. Concerted Proton-Electron Transfer Reactions in Water. Are the Driving Force and Rate Constant Depending on pH When Water Acts as Proton Donor or Acceptor? *J. Am. Chem. Soc.* **2007**, *129*, 5870–5879.

9 Kiefer, P. M.; Hynes, J. T. Kinetic Isotope Effects for Nonadiabatic Proton Transfer Reactions in a Polar Environment. 1. Interpretation of Tunneling Kinetic Isotopic Effects. *J. Phys. Chem. A* **2004**, *108*, 11793–11808.

10 Costentin, C.; Robert, M.; Savéant, J.-M. Electrochemical and Homogeneous Proton-Coupled Electron Transfers: Concerted Pathways in the One-Electron Oxidation of a Phenol Coupled with an Intramolecular Amine-Driven Proton Transfer. *J. Am. Chem. Soc.* **2006**, *128*, 4552–4553.

11 Rhile, I. J.; Markle, T. F.; Nagao, H.; DiPasquale, A. G.; Lam, O. P.; Lockwood, M. A.; Rotter, K.; Mayer, J. M. Concerted Proton-Electron Transfer in the Oxidation of Hydrogen-Bonded Phenols. *J. Am. Chem. Soc.* **2006**, *128*, 6075–6088.

12 Costentin, C.; Robert, M.; Savéant, J. M. Carboxylates as Proton-Accepting Groups in Concerted Proton-Electron Transfers. Electrochemistry of the 2,5-Dicarboxylate 1,4-Hydrobenzoquinone/2,5-Dicarboxy 1,4-Benzoquinone Couple. *J. Am. Chem. Soc.* **2006**, *128*, 8726–8727.

13 Hynes, J. T. Physical chemistry: The peripatetic proton. *Nature* **2007**, *446*, 270–273.

14 Costentin, C.; Louault, C.; Robert, M.; Savéant, J.-M. Evidence for Concerted Proton-Electron Transfer in the Electrochemical Oxidation of Phenols with Water as Proton Acceptor. Tri-*tert*-butylphenol. *J. Am. Chem. Soc.* **2008**, *130*, 15817–15819.

15 Costentin, C.; Louault, C.; Robert, M.; Savéant, J. M. The electrochemical approach to concerted proton-electron transfers in the oxidation of phenols in water. *Proc. Natl. Acad. Sci. U.S.A.* **2009**, *106*, 18143–18148.

16 Bonin, J.; Costentin, C.; Louault, C.; Robert, M.; Routier, M. ; Savéant, J.-M. Intrinsic Reactivity and Driving Force Dependence in Concerted Proton-Electron Transfers to Water Illustrated by Phenol Oxidation. *Proc. Natl. Acad. Sci. U.S.A.* **2010**, *107*, 3367−3372.

17 Sjodin, M.; Irebo, T.; Utas, J. E.; Lind, J.; Merenyi, G.; Akermark, B.; Hammarstrom, L. Kinetic Effects of Hydrogen Bonds on Proton-Coupled Electron Transfer from Phenols. *J. Am. Chem. Soc.* **2006**, *128*, 13076–13083.

18 Krishtalik, L. I. pH-dependent redox potential: how to use it correctly in the activation energy analysis. *Biochim. Biophys. Acta, Bioenerg.* **2003**, *1604*, 13–21.

19 Song, N.; Stanbury, D. M. Proton-Coupled Electron-Transfer Oxidation of Phenols by Hexachloroiridate(IV). *Inorg. Chem.* **2008**, *47*, 11458–11460.

20 (a) Costentin, C.; Robert, M.; Savéant, J.-M.; Teillout, A.-L. Concerted and Stepwise Proton-Coupled Electron Transfers in Aquo/Hydroxo Complex Couples in Water: Oxidative Electrochemistry of $[Os^{II}(bpy)_2(py)(OH_2)]^{2+}$. *ChemPhysChem* **2009**, *10*, 191–198. (b) Costentin, C.; Robert, M.; Savéant, J.-M.; Teillout, A.-L. Concerted proton-coupled electron transfers in aquo/hydroxo/oxo metal complexes: Electrochemistry of $[Os^{II}(bpy)_2py(OH_2)]^{2+}$ in water. *Proc. Natl. Acad. Sci. U.S.A.* **2009**, *106*, 11829–11836.

21 Madhiri, N.; Finklea, H. O. Potential-, pH-, and Isotope-Dependence of Proton-Coupled Electron Transfer of an Osmium Aquo Complex Attached to an Electrode. *Langmuir* **2006**, *22*, 10643–10651.

22 (a) Costentin, C.; Evans, D. H.; Robert, M.; Savéant, J. M.; Singh, P. S. Electrochemical Approach to Concerted Proton and Electron Transfers. Reduction of the Water-Superoxide Ion Complex. *J. Am. Chem. Soc.* **2005**, *127*, 12490–12491. (b) Singh, P. S.; Evans, D. H. Study of the Electrochemical Reduction of Dioxygen in Acetonitrile in the Presence of Weak Acids. *J. Phys. Chem. B* **2006**, *110*, 637–644.

23 Savéant, J. M. Electrochemical Concerted Proton and Electron Transfers. Further Insights in the Reduction Mechanism of Superoxide Ion in the Presence of Water and Other Weak Acids. *J. Phys. Chem. C* **2007**, *111*, 2819–2822.

24 Wang, S.; Singh, P. S.; Evans, D. H. Concerted Proton-Electron Transfer: Effect of Hydroxylic Additives on the Reduction of Benzophenone, 4-Cyanobenzophenone, and 4,4′-Dicyanobenzophenone. *J. Phys. Chem. C* **2009**, *113*, 16686–16693.